

# Solubility of Poly(tetrafluoroethylene-*co*-19 mol % hexafluoropropylene) in Supercritical CO<sub>2</sub> and Halogenated Supercritical Solvents

Cynthia A. Mertdogan,<sup>†</sup> Hun-Soo Byun,<sup>†,‡</sup> Mark A. McHugh,<sup>\*,†</sup> and William H. Tuminello<sup>§</sup>

Department of Chemical Engineering, Johns Hopkins University, Baltimore, Maryland 21218, and Experimental Station, The DuPont Company, Wilmington, Delaware 19880-0356

Received April 16, 1996; Revised Manuscript Received July 2, 1996<sup>®</sup>

**ABSTRACT:** High-pressure cloud-point data are presented for poly(tetrafluoroethylene-*co*-19.3 mol % hexafluoropropylene) (FEP<sub>19</sub>) in CF<sub>4</sub>, C<sub>2</sub>F<sub>6</sub>, C<sub>3</sub>F<sub>8</sub>, C<sub>3</sub>F<sub>6</sub>, CClF<sub>3</sub>, CO<sub>2</sub>, and SF<sub>6</sub> at 118–250 °C and pressures as high as 2700 bar. Cloud-point curves for a given solvent virtually superpose for FEP<sub>19</sub> concentrations between 2 and 10 wt %. It is not possible to dissolve FEP<sub>19</sub> in CO<sub>2</sub> at temperatures less than 185 °C due to strong quadrupolar self-interactions relative to cross-interactions between FEP<sub>19</sub> and CO<sub>2</sub>. The location of the cloud-point curves in pressure–temperature space are directly related to the product of the polarizability and molar density,  $\rho_i\alpha_i$ , of the solvent as determined at the cloud-point pressure at a given temperature. The average of  $\rho_i\alpha_i$  is  $5.14 \times 10^{-24}$  mol  $\pm$  7% for the SCF solvents considered in this study calculated at 200 °C and it is  $5.41 \times 10^{-24}$  mol  $\pm$  7% for all of the solvents except CF<sub>4</sub> and CO<sub>2</sub> at 170 °C. This simple correlation provides a means for estimating cloud-point pressures for nonpolar polymers with nonpolar solvents, or for polar solvents at very high temperatures where polar interactions are diminished. Using this correlation, it is not possible to predict when crystallization may occur or when polar interactions will dictate the phase behavior as observed for CO<sub>2</sub> at temperatures below 185 °C. With one temperature-independent and one temperature-dependent mixture parameter the Sanchez–Lacombe equation of state (SLEOS) is capable of modeling the phase behavior of FEP<sub>19</sub> in the solvents considered in this study except for CO<sub>2</sub> which required two temperature-dependent parameters. It is not possible to even qualitatively model the cloud-point behavior if the two mixture parameters are set to zero. Hence, the utility of the SLEOS is limited since cloud-point data are needed to fix the values and the temperature dependence of the mixture parameters.

## Introduction

Fluoropolymers, and particularly poly(tetrafluoroethylene) (PTFE), have generally been considered resistant to dissolution in most common solvents.<sup>1</sup> Relative to their fluorinated analogs, organic solvents containing hydrogen exhibit lower adsorption on PTFE films and fluorinated copolymers due to the lack of favorable interactions between small hydrogen atoms in the solvent and large, electronegative fluorine atoms in the polymer.<sup>2</sup> Although PTFE is considered insoluble, recent studies have shown that it is possible to dissolve PTFE and its copolymers in many halogenated solvents including tertiary perfluoroamines, perfluorinated olefins, perfluorokerosenes, perfluorinated oils, and poly(hexafluoropropylene oxide) oligomers.<sup>1,3,4</sup> Most of these studies are performed at temperatures near the melting point of PTFE,  $T_{\text{melt}} \sim 330$  °C, and at atmospheric pressure since solid PTFE remains essentially insoluble in these solvents until it melts. Tuminello et al.<sup>5</sup> demonstrate that low-boiling halocarbons, nonsolvents for PTFE at atmospheric pressure, dissolve PTFE at elevated pressures, and they suggest that, for these particular halocarbons, solvent density controls solubility once the PTFE melts. A linear relationship exists between the critical temperature of these low-boiling halocarbons and the cloud-point pressures for their respective PTFE–solvent mixtures. In turn, for two mixtures at the same temperature, a lower pressure is needed to dissolve the PTFE–solvent mixture contain-

ing the solvent with a higher critical temperature since less pressure is required to densify this less-volatile halocarbon.

Recently, Tuminello, Dee, and McHugh<sup>6</sup> presented experimental evidence that carbon dioxide (CO<sub>2</sub>) can dissolve a fluorinated copolymer at high temperatures and high pressures, although only a limited experimental study was performed. DeSimone has reported on the homogeneous solution polymerization of fluoropolymers in supercritical carbon dioxide but has limited the application to amorphous fluoropolymers.<sup>7</sup> The purpose of the present article is to further explore the possibility of using low molecular weight, supercritical fluid (SCF) solvents, such as CO<sub>2</sub>, to dissolve a single, high-melting, crystalline fluorinated copolymer, poly(tetrafluoroethylene-*co*-19.3 mol % hexafluoropropylene) (FEP<sub>19</sub>). The hexafluoropropylene comonomer in FEP<sub>19</sub> disrupts the stereoregularity of the copolymer, which reduces crystallinity and lowers the peak melting point from 327 °C for highly crystalline PTFE to 147 °C for FEP<sub>19</sub>. At the high pressures utilized in this study, crystalline FEP<sub>19</sub> is expected to melt at temperatures much greater than 147 °C due to hydrostatic pressure which is expected to increase the melting temperature at a rate of  $\sim 1.0$  °C/10 bar, the rate observed for PTFE.<sup>6,8</sup> Dispersion-type forces are expected to be the dominant type of intermolecular force of attraction between segments of FEP<sub>19</sub> given that the hexafluoropropylene incorporated into the copolymer backbone exhibits characteristics of nonpolar perfluoropropane. FEP<sub>19</sub> has a weight-average molecular weight of  $\sim 210\,000$ <sup>9</sup> and is end-capped with carboxylic acid groups which amount to approximately 1000 mass-ppm acid groups. Although Radosz and Gregg show that terminal acid groups can have a large impact on the phase behavior

<sup>†</sup> Johns Hopkins University.

<sup>‡</sup> Currently at the Department of Chemical Engineering, Yosu National University, Korea.

<sup>§</sup> DuPont.

<sup>®</sup> Abstract published in *Advance ACS Abstracts*, August 15, 1996.

**Table 1. Physical Properties of the Solvents Used in This Study<sup>a,11-14</sup>**

solvent	mol wt	critical temp (°C)	critical pressure (bar)	critical density (g/cm <sup>3</sup> )	acentric factor	polarizability (cm <sup>3</sup> × 10 <sup>-25</sup> )	dipole moment (Debye)
CF <sub>4</sub>	88.0	-45.6	37.4	0.630	0.177	28.6	0.0
C <sub>2</sub> F <sub>6</sub>	138.0	19.7	29.8	0.622	0.244	47.6	0.0
C <sub>3</sub> F <sub>8</sub>	188.0	71.9	26.8	0.627	0.325	66.7	0.0
C <sub>3</sub> F <sub>6</sub>	150.0	94.0	29.0	0.510	0.191	60.4	0.4
CClF <sub>3</sub>	104.5	28.8	38.7	0.579	0.198	45.8	0.5
CO <sub>2</sub>	44.0	31.0	73.8	0.469	0.225	26.5	0.0
SF <sub>6</sub>	146.1	45.5	37.6	0.735	0.286	54.6	0.0

<sup>a</sup> The acentric factors for C<sub>2</sub>F<sub>6</sub> and C<sub>3</sub>F<sub>6</sub> were calculated using the correlation of Pitzer. The polarizabilities of the halogenated solvents were calculated using the method of Miller and Savchik.<sup>15</sup> The dipole moments of C<sub>3</sub>F<sub>8</sub> and C<sub>3</sub>F<sub>6</sub> are assumed to be equal to those of propane and propylene, respectively. CO<sub>2</sub> also possesses a quadrupole moment of  $-4.3 \times 10^{-26}$  erg<sup>1/2</sup>·cm<sup>5/2</sup> and C<sub>2</sub>F<sub>6</sub> possesses a quadrupole moment of  $-0.65 \times 10^{-26}$  erg<sup>1/2</sup>·cm<sup>5/2</sup>.

of nonpolar polymers,<sup>10</sup> the polymers that they considered had molecular weights only in the range of 10 000. In the present study, the molecular weight of FEP<sub>19</sub> is in excess of 100 000 and, therefore, the small concentration of oligomer acid ends are expected to only mildly influence the phase behavior.

Table 1 lists the properties of the three classes of supercritical fluid (SCF) solvents chosen for this study. The cloud-point behavior of FEP<sub>19</sub> is measured in three nonpolar perfluoroalkanes, tetrafluoromethane (CF<sub>4</sub>), hexafluoroethane (C<sub>2</sub>F<sub>6</sub>), and octafluoropropane (C<sub>3</sub>F<sub>8</sub>); in two polar halocarbons, hexafluoropropylene (C<sub>3</sub>F<sub>6</sub>) and chlorotrifluoromethane (CClF<sub>3</sub>); and in carbon dioxide (CO<sub>2</sub>) and sulfur hexafluoride (SF<sub>6</sub>). Since the dissolution behavior of PTFE was found to resemble that of polyethylene (PE),<sup>1</sup> the cloud-point behavior of FEP<sub>19</sub> in the saturated perfluoroalkanes is expected to parallel that found for PE in normal alkanes, where cloud-point pressures decrease with increasing molecular weight of the alkane.<sup>16-18</sup> Since the experimental apparatus used in this study is capable of operating to kilobar pressures, CF<sub>4</sub> can be used as the base-case perfluoroalkane since it has the lowest molecular weight, polarizability, and critical temperature of the perfluoroalkane family. Relative to CF<sub>4</sub>, the next simplest perfluoroalkane, C<sub>2</sub>F<sub>6</sub>, has an increased molecular weight, polarizability, and critical temperature which means that lower pressures are needed to densify C<sub>2</sub>F<sub>6</sub> and that stronger favorable interactions are expected between C<sub>2</sub>F<sub>6</sub> and nonpolar FEP<sub>19</sub>. Likewise, the trend to lower solution pressures and stronger interactions is expected to continue with C<sub>3</sub>F<sub>8</sub>. The impact of a small solvent dipole moment on the cloud-point behavior of FEP<sub>19</sub> is ascertained by comparing the phase behavior of FEP<sub>19</sub> in C<sub>3</sub>F<sub>6</sub> with that in C<sub>3</sub>F<sub>8</sub>, which has a polarizability similar to that of C<sub>3</sub>F<sub>6</sub>. Likewise, the phase behavior of FEP<sub>19</sub> in CClF<sub>3</sub> is compared to that in C<sub>2</sub>F<sub>6</sub>, which possesses a polarizability similar to that of CClF<sub>3</sub>. CO<sub>2</sub> and SF<sub>6</sub> are also used in this study as these two SCF solvents have experienced recent scrutiny as environmentally acceptable process solvents. The impact of the quadrupole of CO<sub>2</sub> is investigated with a comparison of the phase behavior of FEP<sub>19</sub> in CF<sub>4</sub> with that in CO<sub>2</sub> since both of these solvents have essentially the same polarizability, even though their critical temperatures differ by over 80 °C. SF<sub>6</sub> is a large, totally fluorinated solvent with a modest critical temperature as well as a large polarizability which suggests that SF<sub>6</sub> will be an adequate solvent for FEP<sub>19</sub>.

## Experimental Section

Experimental cloud-point data are obtained by using two distinct high-pressure, variable-volume view cells. Both cells are constructed of Nitronic 50, a high-strength nickel alloy,

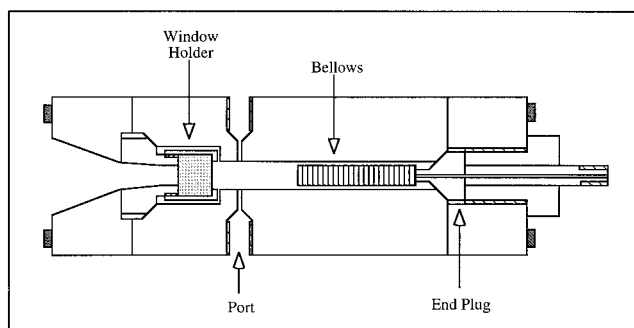


**Figure 1.** Schematic diagram of the high-temperature cell used to obtain cloud-point data in this study.

and are capable of operating to 2750 bar. One of the high-pressure cells, described in detail elsewhere,<sup>19</sup> employs a movable piston with elastomeric O-rings to vary the system pressure. However, the operation of this cell is limited to temperatures slightly in excess of 200 °C due to thermal degradation of the O-rings. Figure 1 shows a schematic diagram of the other high-pressure cell, based on the designs of Buback and Franck,<sup>20</sup> which can operate to temperatures as high as 350 °C since the O-ring seals are replaced with metal cone-and-plug end-cap seals, a Poulter window seal, and a metal bellows. The high-pressure, high-temperature cell (6.35 cm o.d. × 1.03 cm i.d. and ~10 cm<sup>3</sup> working volume) utilizes a 0.95 cm o.d. stainless steel bellows (Standard Bellows Co.) and a 1.59 cm o.d. × 1.27 cm thick sapphire window. The experimental setup and techniques are similar for the two cells.

While being maintained at room temperature, the cell is purged first with nitrogen at pressures of 30–50 bar and then with the solvent of interest at 3–6 bar to remove any entrapped air. Approximately  $(8-16) \pm 0.002$  g of solvent is transferred into the cell, that had been previously loaded with  $(0.3-0.7) \pm 0.002$  g of solid copolymer, depending on the desired weight fraction of polymer in solution. The system pressure is measured to within  $\pm 2.8$  bar and the system temperature is measured to within  $\pm 0.2$  deg, but is maintained to within  $\pm 0.2$  deg below 200 °C and  $\pm 0.4$  deg above 200 °C. The cloud-point pressure is defined as the point at which the solution becomes so opaque that it is no longer possible to see the stir bar in solution. The results obtained with this definition of the cloud point have been compared in our laboratories with results obtained using a laser light setup where the cloud point is defined as the condition of 90% drop off in light transmitted through the solution. The cloud points obtained by both methods gave identical results within the reproducibility of the data. Cloud-point measurements are repeated at least twice at each temperature and are typically reproducible to within  $\pm 5$  bar. The lowest temperature of the cloud-point curves is either the highest operating pressure of the experimental apparatus or the crystallization boundary, whichever comes first.

**Materials.** FEP<sub>19</sub>, hexafluoropropylene, and octafluoropropane were kindly donated by The DuPont Co. More detailed information on the characteristics of FEP<sub>19</sub> are given by Tuminello,<sup>9</sup> where FEP<sub>19</sub> is designated LMFEP-2. The HFP

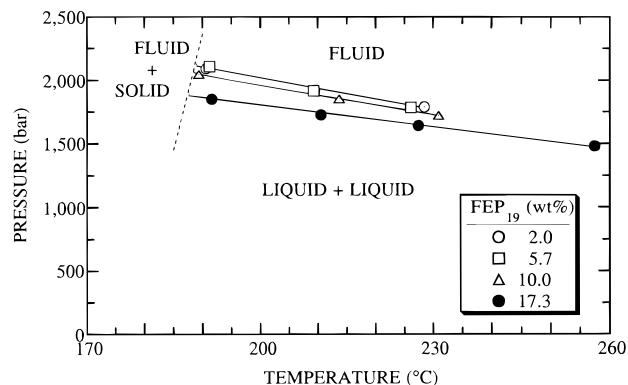


**Figure 2.** Effect of poly(tetrafluoroethylene-*co*-19.3 mol % hexafluoropropylene) (FEP<sub>19</sub>) concentration on the location of the cloud-point curves in CF<sub>4</sub> with the crystallization boundary denoted by the dashed line.

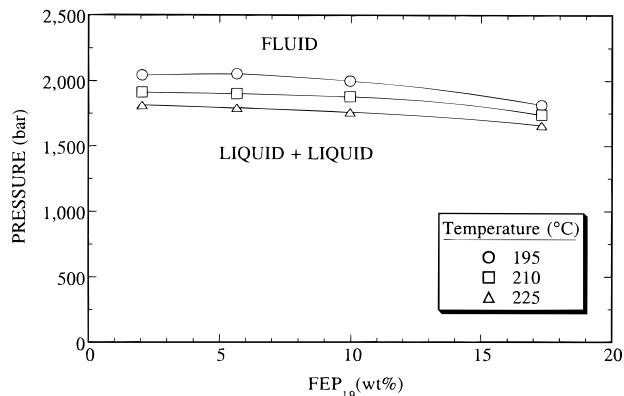
content (19.3 mol %) was determined spectroscopically and the weight-average molecular weight (210 000) was calculated from low strain rate melt viscosity. Carbon dioxide (Bone Dry grade, 99.8% minimum purity) was obtained from Airgas Inc. CClF<sub>3</sub>, CF<sub>4</sub>, C<sub>2</sub>F<sub>6</sub>, and SF<sub>6</sub> (all CP grade, 99.0% minimum purity) were obtained from MG Industries. All of the solvents were used as-received.

## Results and Discussion

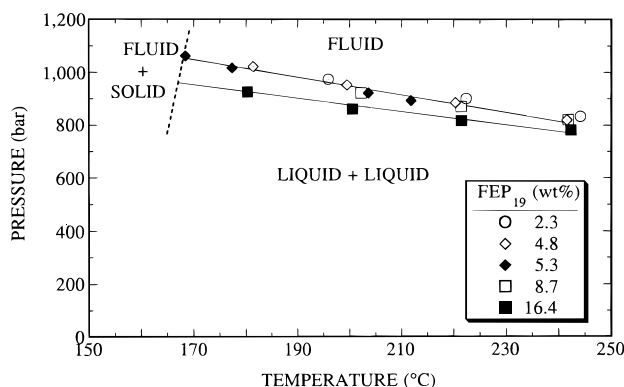
For many of the arguments invoked to explain the data in this study, it is necessary to have an estimate of solvent density at the cloud-point conditions. The Peng–Robinson equation of state<sup>21</sup> is used to calculate the densities of the SCF solvents at the elevated temperatures and pressures used in this study. The cloud-point data of FEP<sub>19</sub> in the supercritical fluorocarbons are presented first, followed by the data for the FEP<sub>19</sub>–nonfluorocarbon solvent systems.

Figure 2 shows the effect of FEP<sub>19</sub> concentration on the cloud-point behavior in CF<sub>4</sub>, the simplest fluoroalkane investigated in this study. The locations of the cloud-point curves are insensitive to FEP<sub>19</sub> concentration in the range of 2–10 wt %; however, the cloud-point curve for 17.3 wt % FEP<sub>19</sub> is at lower pressures than the other three curves. The effect of FEP<sub>19</sub> concentration shown in Figure 2 is consistent with behavior exhibited by hydrocarbon polymer–hydrocarbon solvent systems.<sup>22,23</sup> Although CF<sub>4</sub> is a nonpolar fluoroalkane that has properties similar to those of a repeat unit of FEP<sub>19</sub>, CF<sub>4</sub> has a small polarizability which makes it a very feeble SCF solvent. Given that its critical temperature of  $-45.6^\circ\text{C}$  is very low, CF<sub>4</sub> becomes a highly expanded SCF solvent in the temperature range 180–260 °C, as shown in Figure 2. Thus, very high pressures are needed to obtain sufficient solvent density for CF<sub>4</sub> to solubilize FEP<sub>19</sub>.

Note that the crystallization boundary of FEP<sub>19</sub> in CF<sub>4</sub> occurs at approximately 189 °C at pressures of  $\sim 2000$  bar compared to a peak melting temperature of 147 °C at atmospheric pressure for pure FEP<sub>19</sub>. At temperatures below  $\sim 189^\circ\text{C}$ , solid polymer is observed in solution and it is impossible to obtain a single phase, regardless of pressure. At a starting temperature of 185 °C and a constant pressure of  $\sim 2000$  bar, the temperature must be increased by  $\sim 25$  deg in approximately 10 min to obtain a clear, single phase. The magnitude of this temperature overshoot is similar to the supercooling found for PTFE in non-SCF fluorocarbon solvents.<sup>4</sup> In the presence of solvent at high pressures there are two competing effects that fix the location of the crystallization boundary. One is hydrostatic pres-



**Figure 3.** Pressure–composition isotherms for poly(tetrafluoroethylene-*co*-19.3 mol % hexafluoropropylene) (FEP<sub>19</sub>) in CF<sub>4</sub>.



**Figure 4.** Effect of poly(tetrafluoroethylene-*co*-19.3 mol % hexafluoropropylene) (FEP<sub>19</sub>) concentration on the location of the cloud-point curves in C<sub>2</sub>F<sub>6</sub> with the crystallization boundary denoted by the dashed line.

sure that increases the melting temperature at a rate of  $\sim 1.0$  deg/10 bar, which is the rate observed for PTFE.<sup>6,8</sup> The other effect is the melting point depression of FEP<sub>19</sub> that results from the solubility of CF<sub>4</sub> in the FEP<sub>19</sub>-rich liquid phase. Thus, while 2000 bar of hydrostatic pressure raises the melting point of pure FEP<sub>19</sub> from 147 to  $\sim 347^\circ\text{C}$ , the presence of CF<sub>4</sub> in the FEP<sub>19</sub>-rich liquid phase reduces the temperature of crystallization to  $\sim 189^\circ\text{C}$  at the same pressure.

The data in Figure 2 are replotted as pressure–composition ( $P$ – $x$ ) isotherms in Figure 3. The maximum of these isotherms appears near 2 wt % FEP<sub>19</sub> although the isotherms are reasonably flat at concentrations between 2 and 10 wt % FEP<sub>19</sub>. The trends exhibited in the  $P$ – $x$  isotherms are also apparent for all of the other FEP<sub>19</sub>–solvent systems considered in this study. Therefore, only pressure–temperature cloud-point curves are reported for the other six SCF solvents.

Figure 4 shows the effect of FEP<sub>19</sub> concentration on the cloud-point behavior in the next larger fluoroalkane, C<sub>2</sub>F<sub>6</sub>. These curves follow many of the trends exhibited by the FEP<sub>19</sub>–CF<sub>4</sub> system. Cloud-point pressures are virtually indistinguishable for FEP<sub>19</sub> concentrations in the range of 2–9 wt % over the temperature range 170–245 °C. However, cloud-point pressures of FEP<sub>19</sub> in C<sub>2</sub>F<sub>6</sub> are 700 to 1000 bar lower than those of FEP<sub>19</sub> in CF<sub>4</sub>. While CF<sub>4</sub> has a higher molar density than C<sub>2</sub>F<sub>6</sub> at the same temperature at their respective cloud-point pressures, the large decrease in cloud-point pressure is attributed to the higher polarizability of C<sub>2</sub>F<sub>6</sub> compared to CF<sub>4</sub>. Thus, favorable dispersion forces must dominate density effects in this case, making C<sub>2</sub>F<sub>6</sub> the better solvent of the two. Also note that the crystallization

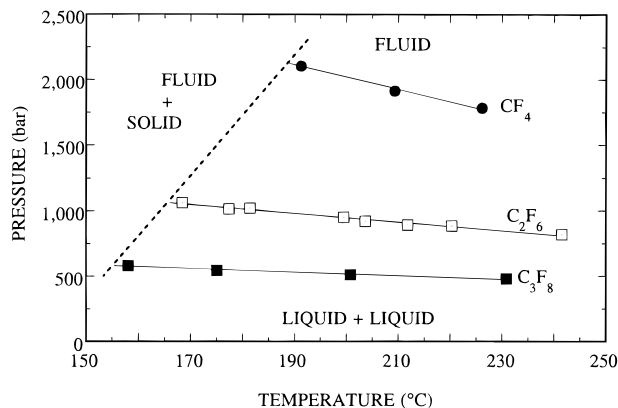


**Figure 5.** Comparison of the cloud-point curves of ~5 wt % poly(tetrafluoroethylene-co-19.3 mol % hexafluoropropylene) in  $\text{CF}_4$ ,  $\text{C}_2\text{F}_6$ , and  $\text{C}_3\text{F}_8$  with the crystallization boundary denoted by the dashed line.

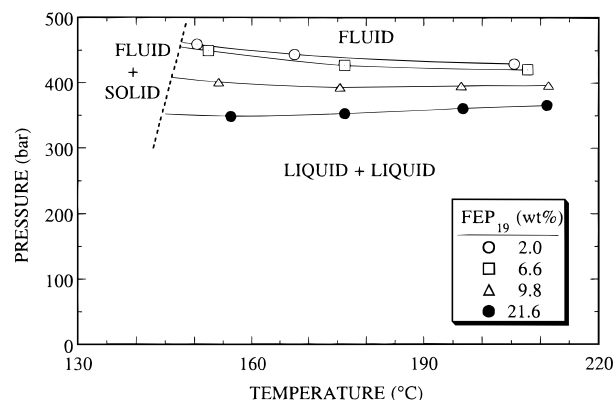
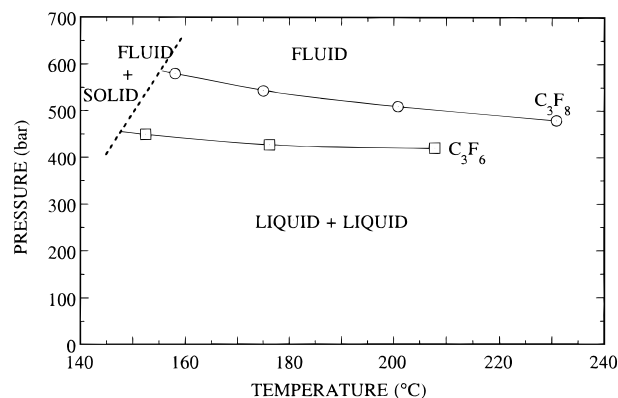


**Figure 6.** Effect of poly(tetrafluoroethylene-co-19.3 mol % hexafluoropropylene) ( $\text{FEP}_{19}$ ) concentration on the location of the cloud-point curves in  $\text{C}_3\text{F}_6$  with the crystallization boundary denoted by the dashed line.

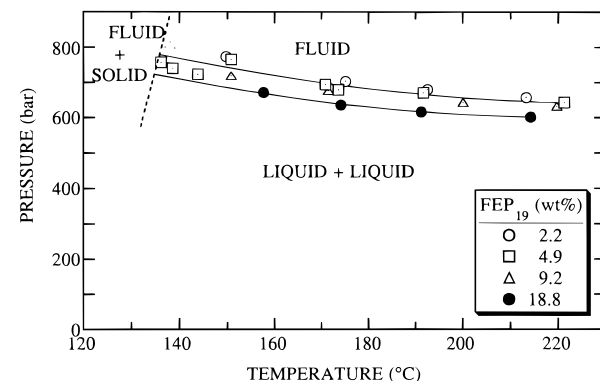
boundary in  $\text{C}_2\text{F}_6$  is ~20 deg lower than in  $\text{CF}_4$  due to the lower cloud-point pressures in  $\text{C}_2\text{F}_6$  and to the likely higher solubility of  $\text{C}_2\text{F}_6$  in the  $\text{FEP}_{19}$ -rich liquid phase.

Figure 5 compares cloud-point curves of 5 wt %  $\text{FEP}_{19}$  in  $\text{CF}_4$ ,  $\text{C}_2\text{F}_6$ , and  $\text{C}_3\text{F}_8$ .  $\text{C}_3\text{F}_8$  has a greater solvent power for  $\text{FEP}_{19}$  than the other two perfluoroalkanes due to its larger polarizability, despite  $\text{C}_3\text{F}_8$  having a lower molar density at the same temperatures at their respective cloud-point pressures. Once again, the favorable dispersion forces dominate density effects, making  $\text{C}_3\text{F}_8$  an even better solvent for  $\text{FEP}_{19}$ . The difference between the cloud-point pressures in  $\text{C}_3\text{F}_8$  compared to  $\text{C}_2\text{F}_6$  is only 300 bar, whereas the difference in  $\text{C}_2\text{F}_6$  relative to  $\text{CF}_4$  is ~1000 bar. The trend of decreasing cloud-point pressure differences with increasing solvent carbon number is similar to that exhibited by polyethylene-normal alkane mixtures.<sup>16,18</sup> The crystallization boundary for the  $\text{C}_3\text{F}_8$  system occurs at ~158 °C, which is ~10 deg lower than that of the  $\text{C}_2\text{F}_6$  system and ~33 deg lower than that of the  $\text{CF}_4$  system. In fact, the high solubility of  $\text{C}_3\text{F}_8$  in the  $\text{FEP}_{19}$ -rich liquid phase, which is implied by the low cloud-point pressures relative to that of the other two fluoroalkanes, virtually offsets the expected 50 deg increase in freezing point of  $\text{FEP}_{19}$  due to hydrostatic pressure alone.

Dipolar forces are expected to have a strong influence on the pressures and temperatures needed to dissolve nonpolar  $\text{FEP}_{19}$ . Figure 6 shows the effect of  $\text{FEP}_{19}$  concentration on the cloud-point behavior in  $\text{C}_3\text{F}_6$ , the polar analog of  $\text{C}_3\text{F}_8$ . As the concentration of  $\text{FEP}_{19}$  increases above ~7 wt %, the cloud-point curves once



**Figure 7.** Comparison of the cloud-point curves of ~5 wt % poly(tetrafluoroethylene-co-19.3 mol % hexafluoropropylene) in  $\text{C}_3\text{F}_8$  and  $\text{C}_3\text{F}_6$  with the crystallization boundary denoted by the dashed line.



**Figure 8.** Effect of poly(tetrafluoroethylene-co-19.3 mol % hexafluoropropylene) ( $\text{FEP}_{19}$ ) concentration on the location of the cloud-point curves in  $\text{CClF}_3$  with the crystallization boundary denoted by the dashed line.

again appear at progressively lower pressures. Figure 7 compares the cloud-point curve for 5 wt %  $\text{FEP}_{19}$  in nonpolar  $\text{C}_3\text{F}_8$  to the curve in slightly polar  $\text{C}_3\text{F}_6$ . The cloud-point curve for the  $\text{C}_3\text{F}_6$  system is ~150 bar lower in pressure at temperatures near 150 °C and ~75 bar lower in pressure at temperatures greater than 190 °C. Also, the crystallization boundary is ~10 deg lower in the slightly polar solvent than in the nonpolar solvent. Both the lower pressures and lower crystallization temperature imply that the slightly polar  $\text{C}_3\text{F}_6$  is a better solvent for nonpolar  $\text{FEP}_{19}$  than is nonpolar  $\text{C}_3\text{F}_8$  which is the opposite trend exhibited by nonpolar polyethylene in propylene and propane.<sup>18</sup> The dipole moment of  $\text{C}_3\text{F}_6$  is expected to enhance  $\text{C}_3\text{F}_6$ - $\text{C}_3\text{F}_6$  intermolecular interactions relative to  $\text{C}_3\text{F}_6$ - $\text{FEP}_{19}$  interactions, which should make  $\text{C}_3\text{F}_6$  a worse solvent for  $\text{FEP}_{19}$  compared to  $\text{C}_3\text{F}_8$ . One possible explanation for this discrepancy is that  $\text{C}_3\text{F}_6$  has a slightly higher critical temperature than  $\text{C}_3\text{F}_8$  which implies that less pressure is required to obtain high densities with  $\text{C}_3\text{F}_6$ . In fact, at the same temperatures at their respective cloud-point pressures, the molar densities of these two solvents are virtually identical.

The impact of a dipole moment is investigated further by determining the phase behavior of  $\text{FEP}_{19}$  in  $\text{CClF}_3$ . Figure 8 shows that the  $\text{FEP}_{19}$  concentration, in the range of 2–9 wt %, has little effect on the location of the cloud-point curve in  $\text{CClF}_3$ . The cloud-point pressures of  $\text{FEP}_{19}$  in slightly polar  $\text{C}_3\text{F}_6$  and  $\text{CClF}_3$  are actually quite similar to those in nonpolar  $\text{C}_3\text{F}_8$  at comparable temperatures since the magnitude of the dipole moments of the two polar solvents are much less

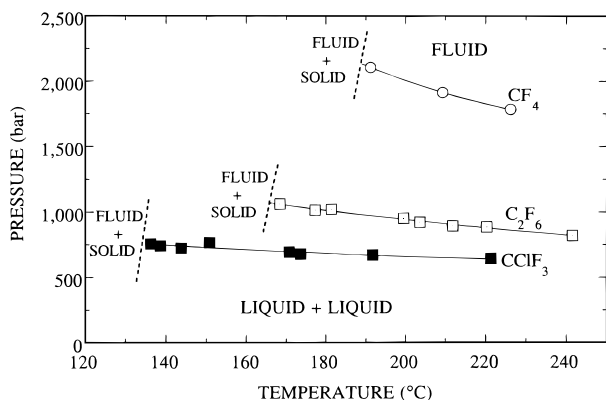


**Figure 9.** Comparison of the cloud-point curves of ~5 wt % poly(tetrafluoroethylene-*co*-19.3 mol % hexafluoropropylene) in  $\text{CF}_4$ ,  $\text{C}_2\text{F}_6$ , and  $\text{CClF}_3$  with the crystallization boundary denoted by the dashed line.

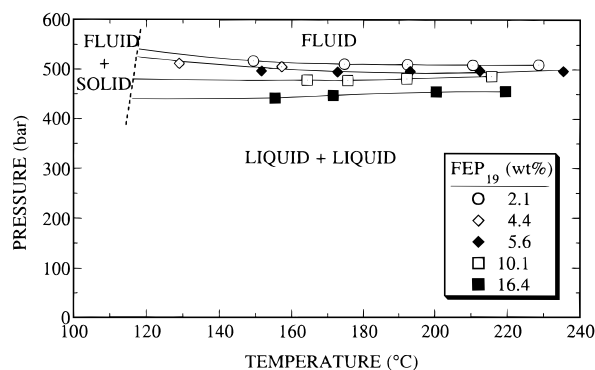


**Figure 10.** Effect of poly(tetrafluoroethylene-*co*-19.3 mol % hexafluoropropylene) ( $\text{FEP}_{19}$ ) concentration on the location of the cloud-point curves in  $\text{SF}_6$  with the crystallization boundary denoted by the dashed line.

than 1 Debye and the effectiveness of these polar moments scales inversely with the square root of the molar volume.<sup>14</sup>  $\text{FEP}_{19}$  in  $\text{CClF}_3$  has slightly higher cloud-point pressures than that in  $\text{C}_3\text{F}_8$  and  $\text{C}_2\text{F}_6$  due to the smaller polarizability of  $\text{CClF}_3$ . Figure 9 compares the cloud-point behavior of  $\text{FEP}_{19}$  in  $\text{CF}_4$ ,  $\text{C}_2\text{F}_6$ , and  $\text{CClF}_3$ . The large decrease in cloud-point pressures of ~1300 bar for the  $\text{CClF}_3$  system relative to the  $\text{CF}_4$  system is a consequence of the larger polarizability of  $\text{CClF}_3$ , despite  $\text{CClF}_3$  having a smaller molar density than  $\text{CF}_4$  at the same temperatures at their cloud-point pressures. On the other hand, the cloud-point pressures for the  $\text{CClF}_3$  system are lower than those for the  $\text{C}_2\text{F}_6$  system even though both of these solvents have essentially the same polarizability. In this case,  $\text{CClF}_3$  has a slightly higher critical temperature compared to  $\text{C}_2\text{F}_6$ , 28.8 °C vs 19.7 °C, which implies that  $\text{CClF}_3$  is easier to densify. Also, the crystallization temperature of the  $\text{CClF}_3$  system, ~138 °C, is 30 deg lower than that of the  $\text{C}_2\text{F}_6$  system. The difference in the solubility behavior of the  $\text{CClF}_3$  and  $\text{C}_2\text{F}_6$  systems may be a density effect.

Sulfur hexafluoride is an interesting solvent for  $\text{FEP}_{19}$  since it has a modest critical temperature and it is nonpolar with a polarizability that is greater than that of  $\text{C}_2\text{F}_6$ . Figure 10 shows that there is little difference in the location of the  $\text{SF}_6$ – $\text{FEP}_{19}$  cloud-point curves at  $\text{FEP}_{19}$  concentrations in the range 2–10 wt %. Figure 11 compares the cloud-point behavior of  $\text{FEP}_{19}$  in  $\text{C}_3\text{F}_8$ ,  $\text{CClF}_3$ , and  $\text{SF}_6$ . The pressures needed to obtain a single phase are lower in  $\text{SF}_6$  except at temperatures greater than 200 °C where cloud-point pressures are lowest for

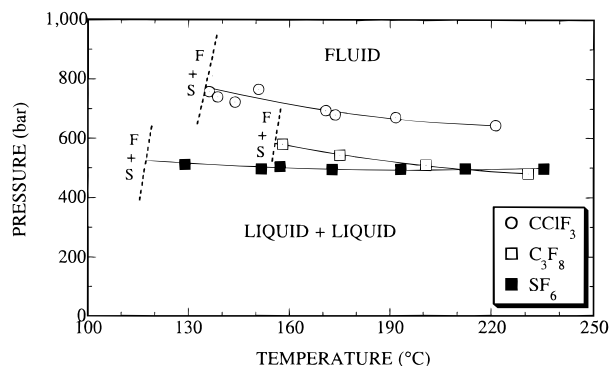


**Figure 11.** Comparison of the cloud-point curves of ~5 wt % poly(tetrafluoroethylene-*co*-19.3 mol % hexafluoropropylene) in  $\text{CClF}_3$ ,  $\text{C}_3\text{F}_8$ , and  $\text{SF}_6$  with the crystallization boundary denoted by the dashed line.

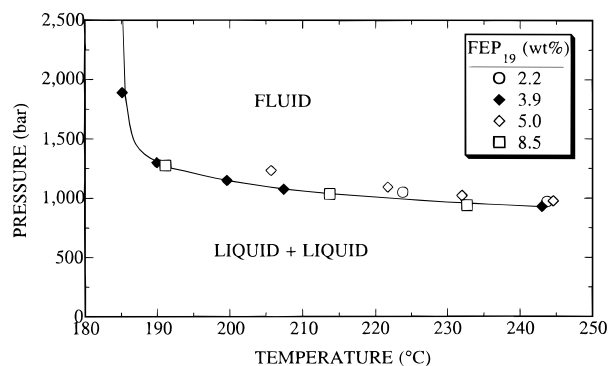


**Figure 12.** Effect of poly(tetrafluoroethylene-*co*-19.3 mol % hexafluoropropylene) ( $\text{FEP}_{19}$ ) concentration on the location of the cloud-point curve in  $\text{CO}_2$ .

the  $\text{C}_3\text{F}_8$ – $\text{FEP}_{19}$  system. The cloud-point curve of the  $\text{SF}_6$  system is closest to, but, generally at lower pressures than, the  $\text{C}_3\text{F}_8$  system. Also, the crystallization boundary in  $\text{SF}_6$  is ~30 deg lower than that in  $\text{C}_3\text{F}_8$ . Although  $\text{SF}_6$  has a smaller polarizability than  $\text{C}_3\text{F}_8$ , it is a better solvent for  $\text{FEP}_{19}$  since the calculated molar density of  $\text{SF}_6$  is approximately 25% greater than that of  $\text{C}_3\text{F}_8$  at the same temperature and at their respective cloud-point pressures. Compared to  $\text{CClF}_3$ ,  $\text{SF}_6$  has a higher polarizability and critical temperature but a lower calculated molar density at cloud-point conditions that is only 85% of that of  $\text{CClF}_3$ . Nevertheless,  $\text{SF}_6$  is a better solvent for  $\text{FEP}_{19}$  due to the favorable dispersion forces between nonpolar  $\text{SF}_6$  and  $\text{FEP}_{19}$  which overpowers the effect of density.

Carbon dioxide is perhaps the most highly touted SCF solvent due to its modest critical temperature, its acceptability and use in the pharmaceutical and food industries, and its so-called environmentally benign characteristics.<sup>24</sup> Figure 12 shows that  $\text{CO}_2$  is a rather feeble solvent for  $\text{FEP}_{19}$  since pressures in the range of 1000 bar are needed to obtain a single phase. As with the other  $\text{FEP}_{19}$ –solvent mixtures, an  $\text{FEP}_{19}$  concentration in the range 2–9 wt % has little effect on the location of the cloud-point curve in  $\text{CO}_2$ . Notice, however, that the  $\text{CO}_2$  cloud-point curve does not intersect a crystallization boundary at low temperatures as did the other  $\text{FEP}_{19}$ –solvent systems. Instead, the  $\text{CO}_2$  cloud-point curve exhibits a steep slope with decreasing temperature near 185 °C. The shape of the  $\text{FEP}_{19}$ – $\text{CO}_2$  cloud-point curve is similar to that found for other polymer–solvent mixtures comprised of a nonpolar component with a polar component,<sup>18,25,26</sup> which suggests that the quadrupole of  $\text{CO}_2$  reduces its solvent

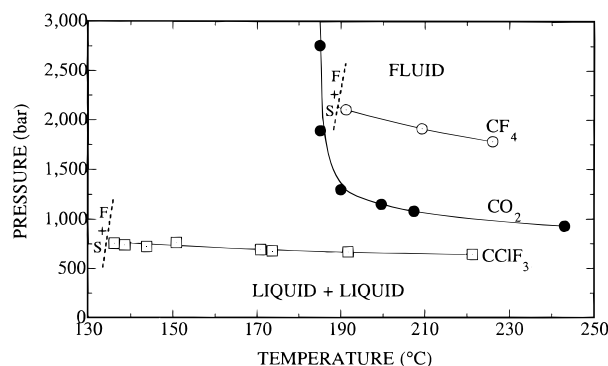


**Figure 13.** Comparison of the cloud-point curves of ~5 wt % poly(tetrafluoroethylene-co-19.3 mol % hexafluoropropylene) in  $\text{CF}_4$ ,  $\text{CO}_2$ , and  $\text{CClF}_3$  with the crystallization boundary denoted by the dashed line.

power for the nonpolar copolymer as the temperature is lowered.

To interpret why carbon dioxide behaves differently than the other SCF solvents, it is instructive to compare the characteristics of the cloud-point curve for  $\text{FEP}_{19}$  in  $\text{CO}_2$  to that in  $\text{CF}_4$  which is nonpolar and has a polarizability close to that of  $\text{CO}_2$ , and to that in  $\text{CClF}_3$ , which has a small dipole moment and a slightly larger polarizability. Figure 13 shows that the cloud-point curves for the  $\text{CO}_2$  and  $\text{CF}_4$  systems almost intersect near 2000 bar and 185 °C where  $\text{FEP}_{19}$  solidifies in  $\text{CF}_4$  but does not solidify in  $\text{CO}_2$ . At 2000 bar and 185 °C, two liquid phases are observed for the  $\text{FEP}_{19}$ – $\text{CO}_2$  system and an increase of only ~2 deg is needed to obtain a single phase. At this same condition, solid polymer is observed in  $\text{CF}_4$  and an increase of ~25 deg is required to obtain a single phase. At temperatures greater than 185 °C, where  $\text{CO}_2$ – $\text{CO}_2$  quadrupolar interactions are reduced,<sup>14</sup> less pressure is required to dissolve  $\text{FEP}_{19}$  in  $\text{CO}_2$  since the calculated molar density of  $\text{CO}_2$  is much greater than that of  $\text{CF}_4$  at the same temperature and pressure. As the temperature is lowered below 185 °C,  $\text{CO}_2$  exhibits enhanced self-interactions, due to its quadrupole moment, that outweigh cross-interactions between  $\text{FEP}_{19}$  and  $\text{CO}_2$ . It is in this temperature range that increased pressure does not help dissolve nonpolar  $\text{FEP}_{19}$  in polar  $\text{CO}_2$ . It is interesting that even though  $\text{CClF}_3$  has a small dipole moment, the  $\text{FEP}_{19}$ – $\text{CClF}_3$  cloud-point curve does not exhibit an extreme negative slope before terminating at a crystallization boundary. It is important to recognize that the impact of the dipole moment and the quadrupole moments scale differently with molar volume.<sup>27</sup> The dipole moment scales inversely with the square root of the molar volume whereas the quadrupole moment scales inversely with the molar volume to the 5/6 power. At temperatures greater than ~190 °C and at the respective cloud-point pressures, the reduced quadrupole moment of  $\text{CO}_2$  is approximately 3 times larger than the reduced dipole moment of  $\text{CClF}_3$  which indicates that  $\text{CO}_2$  is the more polar SCF solvent. Nevertheless, it is surprising that the quadrupolar nature of  $\text{CO}_2$  becomes an important consideration at such high operating temperatures.

Excepting the case with  $\text{CO}_2$  at temperatures below 185 °C, the locations of the cloud-point curves appear to correlate well with solvent density and polarizability. Johnston et al. suggest that solvent density,  $\rho_b$ , or solvent polarizability,  $\alpha_b$ , alone is not a reliable indicator of solvent strength.<sup>28</sup> Rather, they suggest that polarizability times molar density,  $\rho_b\alpha_b$ , is a better indicator

**Table 2.** Characteristic Pure-Component Parameters for the Solvents and Polymer of Interest for Use with the Sanchez–Lacombe Equation of State

component	$T^*$ (K)	$P^*$ (bar)	$\rho^*$ (g/cm <sup>3</sup> )
$\text{CF}_4$	216.3	3134	2.0443
$\text{C}_2\text{F}_6$	276.8	2761	2.0681
$\text{C}_3\text{F}_8$	306.1	2767	2.1363
$\text{CClF}_3$	303.8	3179	1.943
$\text{CO}_2$	305.0	5745	1.510
$\text{SF}_6$	336.4	2497	2.2901
PTFE	641.0	2771	2.134

of solvent strength. The average of  $\rho_b\alpha_b$  is  $5.12 \times 10^{-24}$  mol  $\pm 7\%$  for the SCF solvents considered in this study calculated at 200 °C and at the respective cloud-point pressures. At 170 °C and the respective cloud-point pressures,  $\rho_b\alpha_b$  averages to  $5.41 \times 10^{-24}$  mol  $\pm 7\%$  for all of the solvents except  $\text{CF}_4$  and  $\text{CO}_2$ . Given one set of experimental data, this simple measure of solvent strength provides a means for estimating cloud-point pressures for nonpolar polymers with nonpolar solvents, or for polar solvents at very high temperatures where polar interactions are diminished. Unfortunately, this density–polarizability correlation tool does not predict when crystallization may occur or when polar interactions will dictate the phase behavior as observed for  $\text{CO}_2$  at temperatures below 185 °C. Similar results are expected if solubility parameters are used instead of the density–polarizability approach.

**Modeling.** The Sanchez–Lacombe (SL) equation of state<sup>29</sup> is used to model the  $\text{FEP}_{19}$ –SCF solvent phase behavior presented in this study; the necessary equations are presented in detail elsewhere.<sup>19</sup> The objective of the modeling is to determine whether the SL equation of state, with a minimum number of fitted parameters, can distinguish the difference between the capabilities of the solvents used in this study. Since the majority of the systems investigated here are composed of a nonpolar or slightly polar solvent in solution with a nonpolar copolymer, reasonable results are expected with the SL equation, especially if the mixture parameters are allowed to vary slightly with temperature.

Table 2 lists the three characteristic, pure component parameters,  $T^*$ ,  $P^*$ , and  $\rho^*$ , obtained from a fit of the SL equation to the vapor pressure curve and to saturated liquid densities for  $\text{CF}_4$ ,  $\text{C}_2\text{F}_6$ ,  $\text{C}_3\text{F}_8$ ,  $\text{CClF}_3$ ,  $\text{CO}_2$ , and  $\text{SF}_6$ . The parameters are fit to a minimum of five vapor pressure and liquid density data points<sup>12,13,30,31</sup> to within 50 deg of the critical temperature for each solvent. The calculated critical temperatures for these solvents are ~4% too high; the calculated critical pressures are ~13% too high for  $\text{CF}_4$ ,  $\text{C}_2\text{F}_6$ ,  $\text{C}_3\text{F}_8$ , and  $\text{CClF}_3$ , and they are ~22% too high for  $\text{CO}_2$  and  $\text{SF}_6$ ; the calculated liquid densities are typically 20% too low for all of these solvents. A better fit of the liquid densities could be obtained at the price of a worse fit of the critical temperature and pressure. The  $\text{FEP}_{19}$ – $\text{C}_3\text{F}_8$  system was not modeled since experimental pure component data are not available for  $\text{C}_3\text{F}_8$ . Also, since experimental pure component data are not available for  $\text{FEP}_{19}$ , the characteristic parameters for PTFE are used for the calculations presented here.<sup>6</sup>

Mixing rules are needed to calculate the close-packed molar volume,  $v_{\text{mix}}^*$ , and the characteristic interaction energy,  $\epsilon_{\text{mix}}^*$ , of the mixture. The mixing rule for  $v_{\text{mix}}^*$  is

$$v_{\text{mix}}^* = \sum_{i=1}^2 \sum_{j=1}^2 \varphi_i \varphi_j v_{ij}^* \quad (1)$$

where  $\varphi_i$  and  $\varphi_j$  are volume fractions and the subscripts  $i$  and  $j$  represent the two pure components. The cross term,  $v_{ij}^*$ , is the arithmetic mean of the two pure component characteristic volumes,

$$v_{ij}^* = \frac{1}{2}(v_{ii}^* + v_{jj}^*)(1 - \eta_{ij}) \quad (2)$$

where  $\eta_{ij}$  is a fitted mixture parameter. This parameter accounts roughly for the free volume difference between the solvent and FEP<sub>19</sub>. The mixing rule for  $\epsilon_{\text{mix}}^*$  is

$$\epsilon_{\text{mix}}^* = \frac{1}{v_{\text{mix}}^*} \sum \varphi_i \varphi_j \epsilon_{ij}^* v_{ij}^* \quad (3)$$

where

$$\epsilon_{ij}^* = (\epsilon_{ii}^* \epsilon_{jj}^*)^{0.5} (1 - k_{ij}) \quad (4)$$

in which  $k_{ij}$  is a mixture parameter that accounts for specific binary interactions between components  $i$  and  $j$  not accounted for by the simple geometric-mean average of  $\epsilon_{ij}^*$ .

No attempt is made to determine the pressure–temperature trace of the crystallization boundary. If the polymer fractions were truly “monodisperse”, the cloud point would be the intersection of the pressure–composition ( $P$ – $x$ ) isotherm at an overall concentration of 5 wt % polymer solution.<sup>32–34</sup> Cloud points were calculated at 5 wt % polymer in solution, neglecting the molecular weight distribution of the copolymer. The pressure–temperature trace of the cloud-point curve is obtained by calculating  $P$ – $x$  isotherms to temperatures as low as the crystallization boundary. For the first set of calculations, the mixture parameters  $k_{ij}$  and  $\eta_{ij}$  were each initially set to zero. However, in all cases, the slopes of the calculated cloud-point curves were slightly positive rather than slightly negative, as observed experimentally, and the calculated cloud-point pressures were as much as 1000 bar too high. For the nonpolar copolymer–solvent mixtures considered in this study,  $k_{ij}$  is not expected to be a function of temperature since temperature-independent dispersion forces are the dominant type of interaction in operation. The mixture parameter,  $\eta_{ij}$ , which accounts for differences in the close-packed volumes, is expected to vary with temperature since the density of the solvent changes considerably over the temperature ranges considered in this study.

Since it was not possible to even qualitatively predict FEP<sub>19</sub>–solvent phase behavior with the Sanchez–Lacombe equation of state, the cloud-point curves were fit to determine whether there were any trends in the values of  $k_{ij}$  and  $\eta_{ij}$  from one system to the next. The first step was to obtain a value of  $k_{ij}$  from the best fit of the cloud-point pressure for each system at 190 °C with  $\eta_{ij}$  equal to zero. The resulting  $k_{ij}$ 's obtained in this manner are shown in Figure 14. It is perhaps not too surprising that there appears to be a strong correlation between  $k_{ij}$  and the product of the critical temperature times the critical volume, except for SF<sub>6</sub>. At present we have no reasonable explanation why SF<sub>6</sub> does not follow the correlation given in Figure 14. For each FEP<sub>19</sub>–solvent system a fixed value of  $k_{ij}$  is used and the cloud-point curve is fit by varying  $\eta_{ij}$  with respect to temperature. Figure 15 shows the variation of  $\eta_{ij}$  with temperature for all of the solvents considered here. It should be noted that it was necessary to allow both

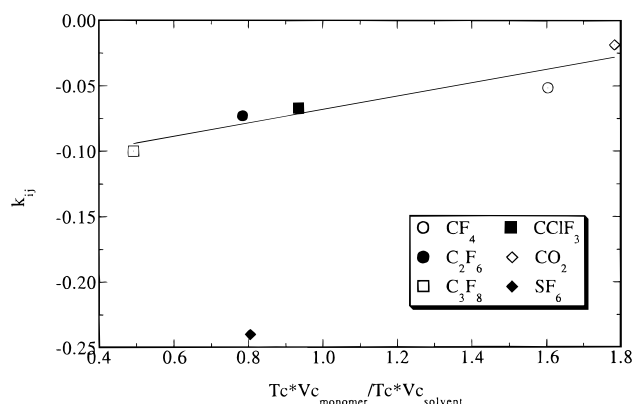


**Figure 14.** Relation of  $k_{ij}$  to critical properties of solvent or monomer, where the critical properties for the monomer were estimated using semi-empirical combining rules<sup>14</sup> between the critical properties of C<sub>2</sub>F<sub>6</sub> and C<sub>3</sub>F<sub>8</sub>.

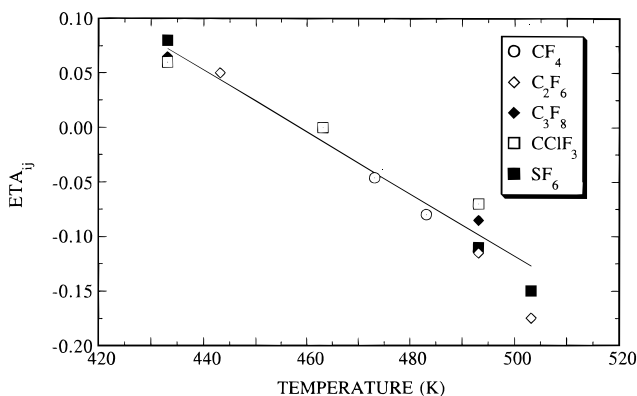


**Figure 15.** Temperature dependence of  $\eta_{ij}$  for each FEP<sub>19</sub>–SCF solvent cloud-point curve. The values are determined with a constant value of  $k_{ij}$  obtained in Figure 14.

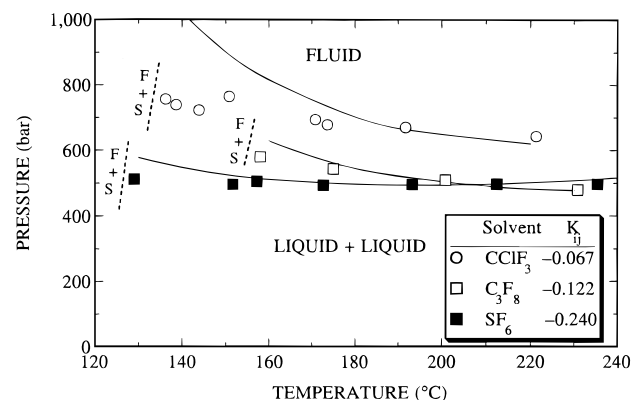


**Figure 16.** Comparison of the calculated and experimental cloud-point curves of ~5 wt % poly(tetrafluoroethylene-*co*-19.3 mol % hexafluoropropylene) in CClF<sub>3</sub>, C<sub>3</sub>F<sub>8</sub>, and SF<sub>6</sub>.

$k_{ij}$  and  $\eta_{ij}$  to vary with temperature to obtain a fit of the FEP<sub>19</sub>–CO<sub>2</sub> system.

Figure 16 shows comparisons of calculated and experimental cloud-point curves for the C<sub>3</sub>F<sub>8</sub>, CClF<sub>3</sub>, and SF<sub>6</sub> systems which are representative of the calculated results obtained with the other solvents. The SL equation of state, with a temperature-dependent  $\eta_{ij}$ , is able to capture the general characteristics of the phase behavior. However, the calculated curves diverge to higher pressures compared to the data at temperatures below 160 °C and above 230 °C. These results suggest that a better fit of the data would be obtained if  $\eta_{ij}$  varied nonlinearly with respect to temperature. Although the Sanchez–Lacombe equation of state can

capture the characteristics of the cloud-point behavior observed in this study, it is not possible to a priori predict the behavior. Further calculational studies are in progress with the statistical associating fluid theory to determine if this model has predictive capabilities for the systems considered here.

## Conclusions

The temperatures and pressures needed to dissolve FEP<sub>19</sub> in supercritical fluorocarbon solvents follows many of the trends exhibited by the solubility behavior of polyethylene in supercritical fluid hydrocarbon solvents. With members of the fluoroalkane family, the FEP<sub>19</sub>–fluoroalkane cloud-point pressure decreases substantially going from CF<sub>4</sub> to C<sub>2</sub>F<sub>6</sub>, and less so from C<sub>2</sub>F<sub>6</sub> to C<sub>3</sub>F<sub>8</sub>. The cloud-point pressures in slightly polar C<sub>3</sub>F<sub>8</sub> and CClF<sub>3</sub> are similar to those in nonpolar C<sub>3</sub>F<sub>8</sub> at comparable temperatures since the magnitude of the dipole moments of the two polar solvents are much less than 1 Debye and the effectiveness of these polar moments scale inversely with the square root of the molar volume. SF<sub>6</sub> is perhaps the most effective SCF solvent for FEP<sub>19</sub> due to its large polarizability and high density relative to the other SCF solvents considered here.

Compared to the other SCF solvents, CO<sub>2</sub> was the worst SCF solvent for FEP<sub>19</sub> at temperatures less than 185 °C due to strong quadrupolar self-interactions of CO<sub>2</sub> relative to cross-interactions between FEP<sub>19</sub> and CO<sub>2</sub>. The FEP<sub>19</sub>–CO<sub>2</sub> cloud-point curve exhibits a steep increase in pressure near 185 °C, which means that increasing CO<sub>2</sub> density does not help dissolve FEP<sub>19</sub>. The cloud-point behavior in CO<sub>2</sub> is attributed to the large quadrupole moment of CO<sub>2</sub> which makes it a polar solvent that is not effective at dissolving a nonpolar copolymer.

Solvent density is not necessarily the defining criteria when estimating whether a nonpolar polymer will dissolve in a supercritical fluid, especially in CO<sub>2</sub>. Johnston et al. suggest that the polarizability per molar volume is a better indicator of solvent strength than solvent density or solvent polarizability alone.<sup>28</sup> In fact, this simple measure of solvent strength provides a means for estimating cloud-point pressures for the perfluoropolymer–SCF solvent systems in this study, although the correlation does not predict when polar interactions will dictate the phase behavior or when crystallization may set in.

The Sanchez–Lacombe equation of state is capable of predicting the phase behavior of the perfluorocopolymer in nonpolar solvents if the mixture parameters are allowed to vary with temperature. The dilemma with this approach is that mixture data are needed to obtain a reasonable estimate of the two mixture parameters,  $\eta_{ij}$  and  $k_{ij}$ . The cloud-point curves predicted by the Sanchez–Lacombe equation of state deviate from experimental results at temperatures below 160 °C and above 220 °C. In addition, the Sanchez–Lacombe equation of state is only able to model the phase behavior of the CO<sub>2</sub>–FEP<sub>19</sub> system if both mixture parameters are allowed to vary with temperature.

**Acknowledgment.** C.A.M. and M.A.M. acknowledge the National Science Foundation for support of this project under Grant CTS-9500489.

## References and Notes

- (1) Smith, P.; Gardner, K. H. *Macromolecules* **1985**, *18*, 1222.
- (2) Starkweather, H. W. *Macromolecules* **1977**, *10*, 1161.
- (3) McCain, G. H.; Covitch, M. J. *J. Electrochem. Soc.* **1984**, *131*, 1350.
- (4) Tuminello, W. H.; Dee, G. T. *Macromolecules* **1994**, *27*, 669.
- (5) Tuminello, W. H.; Brill, D. J.; Walsh, D. J.; Paulaitis, M. E. *J. Appl. Polym. Sci.* **1995**, *56*, 495.
- (6) Tuminello, W. H.; Dee, G. T.; McHugh, M. A. *Macromolecules* **1995**, *28*, 1506.
- (7) DeSimone, J. M.; Guan, Z.; Elsbernd, C. S. *Science* **1992**, *257*, 945.
- (8) Zoller, P. *J. Appl. Polym. Sci.* **1978**, *22*, 633.
- (9) Tuminello, W. H. *Int. J. Polym. Anal. Characterization* **1996**, *2*, 141.
- (10) Gregg, C. J.; Stein, F. P.; Radosz, M. *Macromolecules* **1994**, *27*, 4972.
- (11) Reid, R. C.; Prausnitz, J. M.; Poling, B. E. *The Properties of Gases and Liquids*, 4th ed.; McGraw-Hill: New York, 1987.
- (12) Braker, W.; Mossman, A. L. *Matheson Gas Data Book*, 6th ed.; Matheson: Lyndhurst, NJ, 1980.
- (13) Anon. *Gas Encyclopedia: L'Air Liquide*, Division Scientifique Elsevier Scientific Publishing Co.: Amsterdam, The Netherlands, 1976.
- (14) Prausnitz, J. M.; Lichtenthaler, R. N.; de Azevedo, E. G. *Molecular Thermodynamics of Fluid-Phase Equilibria*, 2nd ed.; Prentice-Hall: Englewood Cliffs, NJ, 1986.
- (15) Miller, K. J.; Savchik, J. A. *J. Am. Chem. Soc.* **1979**, *101*, 7206.
- (16) Ehrlich, P.; Kurpen, J. J. *J. Polym. Sci., Part A* **1963**, *1*, 3217.
- (17) Ehrlich, P.; Mortimer, G. A. *Adv. Polym. Sci.* **1970**, *7*, 386.
- (18) Hasch, B. M.; Meilchen, M. A.; Lee, S.-H.; McHugh, M. A. *J. Polym. Sci., Part B: Polym. Phys.* **1992**, *30*, 1365.
- (19) Meilchen, M. A.; Hasch, B. M.; McHugh, M. A. *Macromolecules* **1991**, *24*, 4878.
- (20) Buback, M.; Franck, E. U. *Ber. Bunsen-Ges. Phys. Chem.* **1972**, *76*, 350.
- (21) Peng, D. Y.; Robinson, D. B. *Ind. Eng. Chem. Fundam.* **1976**, *15*, 59.
- (22) Allen, G.; Baker, C. H. *Polymer* **1965**, *6*, 181.
- (23) Irani, C. A.; Cozewith, C. *J. Appl. Polym. Sci.* **1986**, *31*, 1879.
- (24) McHugh, M. A.; Krukonis, V. J. *Supercritical Fluid Extraction: Principles and Practice*, 2nd ed.; Butterworth Publishers: Stoneham, MA, 1994.
- (25) LoStracco, M. A.; Lee, S.-H.; McHugh, M. A. *Polymer* **1993**, *35*, 3272.
- (26) Lee, S.-H.; LoStracco, M. A.; Hasch, B. M.; McHugh, M. A. *J. Phys. Chem.* **1994**, *98*, 4055.
- (27) Jonah, D. A.; Shing, K. S.; Venkatasubramanian, V.; Gubbins, K. E. Molecular Thermodynamics of Dilute Solutes in Supercritical Solvents. In *Chemical Engineering at Supercritical Fluid Conditions*; Paulaitis, M. E., Penninger, J. M. L., Gray, R. D., Jr., Davidson, P., Eds.; Ann Arbor Science: Ann Arbor, MI, 1983; pp 221–244.
- (28) Johnston, K. P.; Sunwook, K.; Combes, J. Spectroscopic Determination of Solvent Strength and Structure in SCF Mixtures: A Review. In *Supercritical Fluid Science and Technology*; Johnston, K. P., Penninger, J. M. L., Eds.; ACS Symposium Series; American Chemical Society: Washington, DC, 1989; p 52.
- (29) Sanchez, I. C.; Lacombe, R. H. *Macromolecules* **1978**, *11*, 1145.
- (30) Rabinovich, V. A., Ed. *Thermophysical Properties of Matter and Substances*; Standards Publishers: Moscow, 1971; Vol. 4.
- (31) Gilgen, R.; Kleinrahm, R.; and Wagner, W. *J. Chem. Thermodyn.* **1992**, *24*, 953.
- (32) Koningsveld, R.; Staverman, A. J. *J. Polym. Sci., Polym. Phys. Ed.* **1968**, *6*, 305.
- (33) Koningsveld, R.; Staverman, A. J. *J. Polym. Sci., Polym. Phys. Ed.* **1968**, *6*, 325.
- (34) Koningsveld, R.; Staverman, A. J. *J. Polym. Sci., Polym. Phys. Ed.* **1968**, *6*, 349.